CellPress
PARTNER JOURNAL

Molecular Plant
Research Article

Venus Flytrap HKT1-Type Channel Provides for Prey Sodium Uptake into Carnivorous Plant Without Conflicting with Electrical Excitability

J. Böhm[1,5], S. Scherzer[1,5], S. Shabala[2], E. Krol[1], E. Neher[3,4], T.D. Mueller[1,*] and R. Hedrich[1,*]

[1]Julius-von-Sachs Institute, Department for Molecular Plant Physiology and Biophysics, University of Würzburg, Julius-von-Sachs Platz 2, 97082 Würzburg, Germany

[2]School of Land and Food, University of Tasmania, Hobart TAS 7001, Australia

[3]Zoology Department, College of Science, King Saud University, PO Box 2455, Riyadh 11451, Saudi Arabia

[4]Department for Membrane Biophysics, Max Planck Institute for Biophysical Chemistry, 37077 Goettingen, Germany

[5]These authors contributed equally to this article.

***Correspondence: R. Hedrich (hedrich@botanik.uni-wuerzburg.de), T.D. Mueller (mueller@botanik.uni-wuerzburg.de)**

http://dx.doi.org/10.1016/j.molp.2015.09.017

ABSTRACT

The animal diet of the carnivorous Venus flytrap, *Dionaea muscipula*, contains a sodium load that enters the capture organ via an HKT1-type sodium channel, expressed in special epithelia cells on the inner trap lobe surface. DmHKT1 expression and sodium uptake activity is induced upon prey contact. Here, we analyzed the HKT1 properties required for prey sodium osmolyte management of carnivorous *Dionaea*. Analyses were based on homology modeling, generation of model-derived point mutants, and their functional testing in *Xenopus* oocytes. We showed that the wild-type HKT1 and its Na^+- and K^+-permeable mutants function as ion channels rather than K^+ transporters driven by proton or sodium gradients. These structural and biophysical features of a high-capacity, Na^+-selective ion channel enable *Dionaea* glands to manage prey-derived sodium loads without confounding the action potential-based information management of the flytrap.

Key words: sodium channel, HKT1, *Dionaea muscipula*, action potential, glands, sodium uptake

Böhm J., Scherzer S., Shabala S., Krol E., Neher E., Mueller T.D., and Hedrich R. (2016). Venus Flytrap HKT1-Type Channel Provides for Prey Sodium Uptake into Carnivorous Plant Without Conflicting with Electrical Excitability. Mol. Plant. **9**, 428–436.

INTRODUCTION

The Darwin plant *Dionaea muscipula* has developed bilobed traps at the leaf tip to allow the capture of small animals. This insect-dominated diet enables the Venus flytrap to overcome the limitations of its soil nutrient-poor habitats. Insects in search of food are attracted by odorants produced by the flytrap (Kreuzwieser et al., 2014), and when visiting the capture organ they inadvertently stimulate mechanosensitive trigger hairs, causing the firing of action potentials (APs). Two consecutive APs result in the release of viscoelastic energy stored in the peculiar biomechanics of the capture organ. The trap closes within a fraction of a second, trapping the visitor (Forterre et al., 2005; Escalante-Perez et al., 2014). By trying to escape the cage, the prey animal repeatedly touches the mechanical sensors, stimulating the capture organ to fire further APs. This ongoing electrical excitation causes the closed trap to hermetically seal and flood the resulting green stomach with a digestive enzyme cocktail (Böhm et al., 2016). During the absorption phase, macromolecule degradation products and minerals derived from the prey are internalized by the trap (Scherzer et al., 2013; Kruse et al., 2014; Gao et al., 2015; Scherzer et al., 2015). In non-carnivorous plants, such minerals are only accessible from the soil and are taken up by the roots in a highly selective manner. Sodium that is toxic in high concentrations is mostly left behind in glycophytes and deposited in halophytes (Shabala et al., 2014). In contrast, *D. muscipula* gland cells take up sodium from digested sodium-rich insects, and we have very recently identified the molecular nature of the flytrap-associated Na^+ transport entity as an ortholog of the Trk/Ktr/HKT family (Böhm et al., 2016). When the corresponding flytrap gene was expressed in *Xenopus* oocytes, the recorded Na^+ dependent currents carried the hallmark features of a sodium channel.

Published by the Molecular Plant Shanghai Editorial Office in association with Cell Press, an imprint of Elsevier Inc., on behalf of CSPB and IPPE, SIBS, CAS.

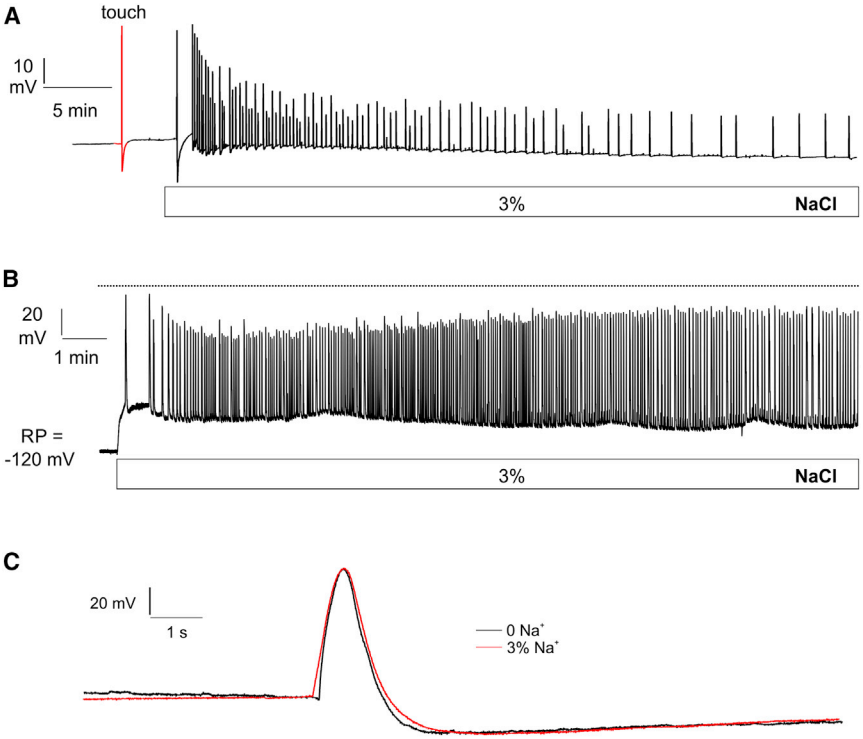

Figure 1. *In Vivo* Measurement of Electrical Excitability of the Venus Flytrap.
(A) Surface potential of Venus flytrap revealed AP firing in response to touch and 3% NaCl treatment.
(B) Membrane voltage recording of impaled *Dionaea* glands exposed to 3% NaCl. This near seawater concentration evoked spontaneous electrical activity with up to 20 APs/min.
(C) Membrane voltage recording of impaled *Dionaea* glands in the absence of Na^+ (black) and presence of 510 mM Na^+ (red). Mechanical stimulation of a trigger hair resulted in firing of APs, which did not differ clearly in amplitude and profile. Representative APs are shown.

Given that distinct serine–glycine polymorphisms in certain members of the Trk/Ktr/HKT family have been associated with proton- and sodium-driven potassium co-transport, we asked how HKT1 mutations of polymorphic sites affect sodium channel function in *Dionaea*. To answer this question, a structure model of the DmHKT1 sodium-selective pore was obtained by homology modeling, and serine residue mutants were generated and functionally analyzed. Thus, we reveal and discuss the transport features of the sodium-selective DmHKT1 channel.

RESULTS

High Saline Conditions Induce Self-Sustained Oscillatory Electrical Activity

DmHKT1 is particularly expressed in digesting glands, known to be responsible for nutrient and mineral uptake. Seawater-like sodium loads are known to be toxic for growth and development in non-halophytic plants (Luan et al., 2009). To study the response of this halophyte-like behavior, we exposed glands to the salinities that halophytes can experience, and followed the plasma membrane electrical responses. Exposure to Na^+ concentrations up to 60 mM Na^+ depolarized the gland cells from −140 to −60 mV (Supplemental Figure 1A), thereby crossing the AP threshold of about −100 mV (Beilby, 2007). This resulted in single APs (Supplemental Figure 1A). When increasing the sodium concentration to near seawater levels of 3% (510 mM), Balotin and Dipalma (1962) observed "spontaneous action potential firing induced in the leaf of *Dionaea*." Reconstructing this scenario enabled us to follow the membrane electrical response resulting from exposure to high salinity using attached voltage-recording surface electrodes and intra-gland cell microelectrodes. Prior to saline treatment, APs in resting traps were elicited by bending a touch-sensitive trigger hair (Figure 1A). Upon exposure to 3% NaCl, the gland cells depolarized by about 30 mV from their resting state of −120 to −140 mV (Figure 1B), superimposed by single APs. With continuing high saline stimulation, multiple APs appeared, the frequency of firing increased and, after about 1 min, the gland cells entered a phase dominated by a self-sustained oscillatory electrical activity (Figure 1A and 1B). In this phase, the intracellular voltage-recording electrodes monitored up to 20 APs per minute. In contrast to animal nerve cells, the size and profile of these APs did not change significantly, even when traps were exposed to 510 mM Na^+. This indicates that Na^+ fluxes neither participate in nor influence the characteristic shape of the AP (Figure 1C).

Sodium Transport via DmHKT1 Is Not Coupled to Fluxes of Counterions

Certain homologs of the archetype Trk/Ktrs, such as plant HKTs, are capable of transporting sodium ions (Hauser and Horie, 2010; Waters et al., 2013). Based on alignments with selected Trk/Ktr/HKT protein sequences from bacteria and plants (Corratge-Faillie et al., 2010; Hauser and Horie, 2010; Ali et al., 2012; Gomez-Porras et al., 2012), we analyzed the DmHKT1 phylogenetic relationship with other Trk/Ktr/HKT proteins and classified the *Dionaea* channel as a member of the HKT subclass 1, with closest homology to HKT1.1 and HKT1.2 from eucalyptus (Böhm et al., 2016). Interestingly, wheat TaHKT1 (now grouped in subclass two renamed TaHKT2; Platten et al., 2006), when expressed in the *Xenopus* oocyte system, was found to couple K^+ uptake to H^+, as well as Na^+ influx in a co-transporter-like manner (Schachtman and Schroeder, 1994; Rubio et al., 1995). In addition, HKT from rice has been proposed to transport calcium ions (Lan et al., 2010; Horie et al., 2011).

To quantify the kinetics of sodium transport through gland cells, as well as to test for Na^+/K^+ flux coupling, we used the microelectrode ion flux measuring (MIFE) technique (Shabala et al., 1997, 2006). In the presence of 0.2 mM K^+, we increased the extracellular Na^+ concentration stepwise from 0 to 50 mM and determined the net flux changes of the two cations. When this experimental scenario was applied to non-stimulated traps, no

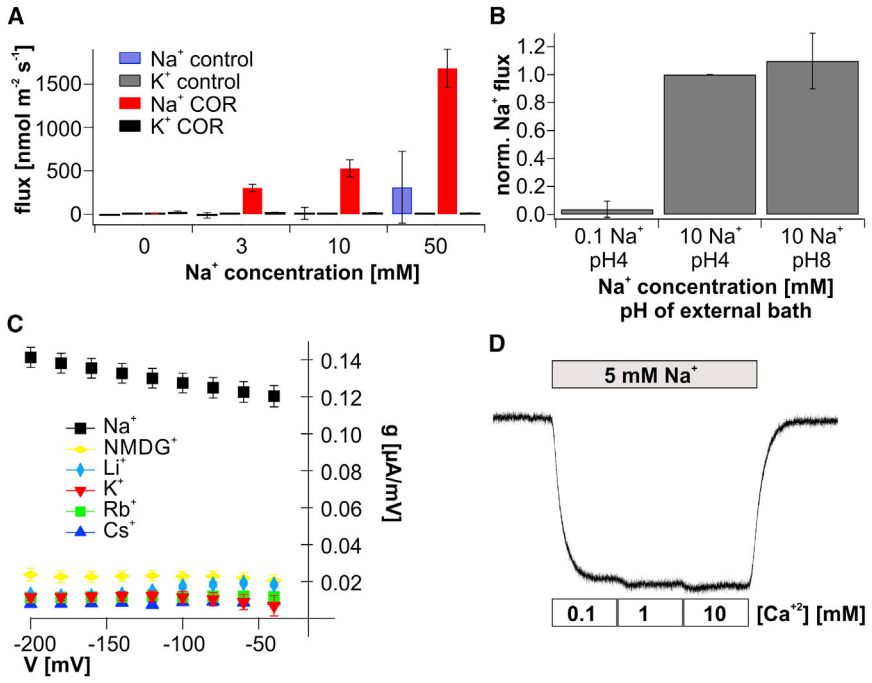

Figure 2. DmHKT1-Driven Na^+ Flux Is Not Coupled to Other Ions.

(A) In MIFE experiments with unstimulated and COR-treated *Dionaea* traps, net Na^+ and K^+ influxes were measured simultaneously under the indicated external Na^+ concentrations. Unstimulated traps under these conditions showed only a small Na^+ uptake of 310 ± 415 nmol m^{-2} s^{-1}. Only stimulated traps revealed a clear Na^+ influx, even under low external sodium concentrations, which increases up to 1683 ± 218 nmol m^{-2} s^{-1} with 50 mM external NaCl. K^+ influx was not significantly affected by a change in the external Na^+ concentration in either unstimulated or COR-treated traps ($n \geq 7$, mean ± SD; $P > 0.5$, one-way ANOVA).

(B) Na^+ influx in *Dionaea* glands is H^+-independent. Normalized Na^+ fluxes from COR-stimulated Venus flytraps were measured in low (0.1 mM; left) and high (10 mM; middle) NaCl concentrations at a pH of 4. Under low external NaCl, the Na^+ influx was only 3.7% ± 5.8% of that in the high external sodium. Increasing the external pH from 4 to 8 (without changing Na^+ concentration; right) did not significantly influence the Na^+ flux (109% ± 19%) ($n \geq 7$, mean ± SD; $P > 0.5$ by one-way ANOVA).

(C) For different monovalent cations at a concentration of 100 mM, the chord conductance was calculated and plotted against the applied voltage range of −40 to −200 mV ($n = 4$, mean ± SD). DmHKT1 was only permeable for sodium.

(D) DmHKT1-mediated inward currents in 5 mM NaCl of a representative *Xenopus* oocyte when the membrane was clamped to −140 mV. The current amplitude did not change significantly by applying Ca^{2+} concentrations of 0.1, 1, and 10 mM (as indicated).

concentration-dependent fluxes of either Na^+ or K^+ were observed. Only when traps were pre-treated with the prey surrogate coronatine (COR) was the increase in external Na^+ level followed by a concentration-dependent influx of sodium ions (Figure 2A). Importantly, the K^+ flux remained unaffected under these conditions, indicating that Na^+ and K^+ fluxes are not coupled to each other.

To determine whether Na^+ transport in gland cells is coupled to a proton flux, we varied the external proton concentrations during *in planta* current-clamp measurements. As depicted in Supplemental Figure 1A, the sodium-induced depolarization triggered at pH 6 remained unaffected when the pH was shifted to 4 and *vice versa*. That the MIFE-detected net sodium flux into stimulated traps remained unaffected by a 10 000-fold change in the proton-motive force (Figure 2B) demonstrates that *Dionaea* gland cells operate an electrogenic Na^+ flux as opposed to H^+/Na^+ co-transport.

When we determined the chord conductance of DmHKT1 expressed in oocytes, we found no conductance toward any monovalent cation, apart from Na^+ (Figure 2C). A near Nernstian behavior of a ~55-mV shift in reversal potential per 10-fold change in extracellular Na^+ concentration (Böhm et al., 2016) is in line with our notion for DmHKT1 operating as a sodium-selective ion channel. Also, the sodium-driven current in DmHKT1-expressing oocytes was not affected by pH changes between values of 4, 6, and 8 (Supplemental Figure 1B). Thus, in the heterologous expression system, DmHKT1 functions similarly to the pH-independent Na^+-selective uptake system of *Dionaea* glands, as characterized herein. Furthermore, the sodium influx in DmHKT1 oocytes was rather insensitive to the addition of calcium to the extracellular medium (Figure 2D). This result indicates that DmHKT1-based Na^+ transport neither is modulated by Ca^{2+} ions nor is the *Dionaea* sodium channel itself permeable to Ca^{2+}.

A Pore Mutation Alters the Conductance of *Dionaea* Sodium Channel Toward Potassium

The findings described above document that the flytrap HKT1 does not represent a co-transporter coupling Na^+ fluxes to those of K^+, H^+, or Ca^{2+}. In this respect, DmHKT1 seems to share its Na^+ selectivity with the Trk/Ktr/HKT-type isoforms grouped in subfamily 1 (Ali et al., 2012; Gomez-Porras et al., 2012). A characteristic of all members of this subfamily is that they carry a serine residue in their first pore loop. In contrast, K^+-permeable Trk/Ktr/HKTs, such as the wheat, barley, and rice orthologs belonging to subfamily 2, frequently have a glycine in the respective position (Supplemental Figure 2). When this particular serine residue in *Dionaea* HKT1 was replaced by glycine, the Na^+ conductance (in 100 mM Na^+ and at $V_m = -140$ mV) dropped by about 75%. In addition, the mutant channel gained a pronounced conductance for K^+ (Figure 3A). When increasing the KCl concentration stepwise to 100 mM, maximal conductance of the S84G was reached at 50 mM K^+ (Figure 3B). This effect could be related to the K^+ self-inhibition known from ion channels in the animal system (Sheng and Kleyman, 2003) and from the K^+/Na^+ transporter (HvHKT2; 1) of barley (Mian et al., 2011). Because of this self-inhibition effect under high K^+ concentrations (Figure 3B), currents mediated by the mutant were of similar amplitude in either 100 mM Na^+- or K^+-based media (Figure 3A). When

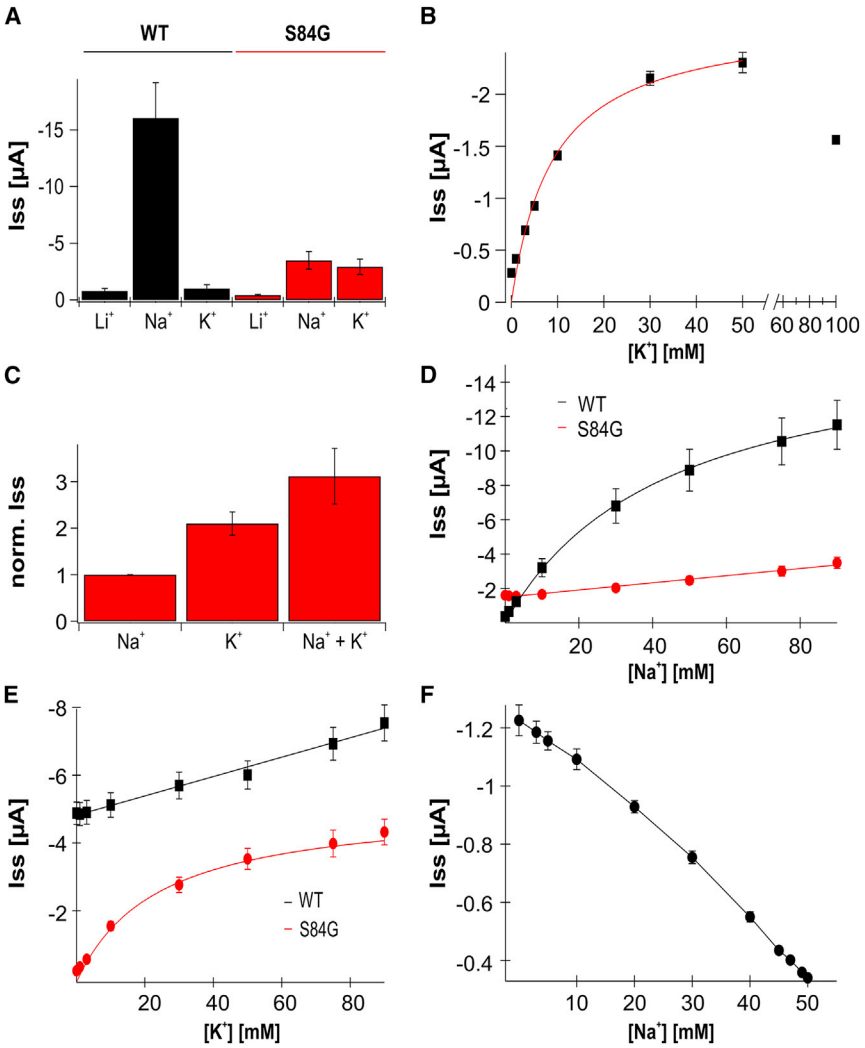

Figure 3. Altered Conductance and Affinity in the DmHKT1 S84G Mutant.

(A) Steady-state currents (Iss) of DmHKT1 wild-type (WT) and S84G-expressing oocytes measured at −140 mV and in 100 mM of the indicated cations (n = 4, mean ± SD).

(B) Steady-state currents (Iss) of DmHKT1 S84G at −140 mV were monitored in and plotted against increasing K^+ concentrations up to 100 mM (please note different scaling). The current response reached a maximum at 50 mM KCl and with higher concentrations, the K^+ inward currents declined. Currents up to 50 mM K^+ could be fitted with the Michaelis–Menten equation revealing a K_m value of 9.01 ± 1.99 mM K^+ (n = 5, mean ± SD).

(C) By applying 10 mM NaCl, 10 mM KCl, and a combination of 10 mM of each cation at −140 mV, S84G-mediated currents under combined ion conditions were the sum of the current responses to each cation alone (n = 5, mean ± SD).

(D) Steady-state currents (Iss) of the WT DmHKT1 and the mutant S84G were monitored in bath solutions containing 10 mM KCl and a stepwise increase in sodium concentrations. WT-mediated currents could be fitted with the Michaelis–Menten equation, whereas the current response of S84G proceeded in a linear-dependent manner ($n \geq 4$, mean ± SD).

(E) In inverse experiments, steady-state currents (Iss) of the WT and the mutant S84G were measured in 10 mM NaCl and a stepwise increase in potassium concentrations ($n \geq 4$, mean ± SD). The resulting currents showed behavior opposite to that shown in **(D)**.

(F) The AMFE of S84G-expressing cells (n = 4, mean ± SD) analyzed in increased Na^+ concentrations, supplemented with K^+ to a final concentration of 50 mM. To maintain the ionic strength, 50 mM LiCl was used. The steady-state currents (Iss) at −140 mV were plotted against the sodium concentration.

decreasing the concentrations of the alkali cations K^+ and Na^+ from 100 to 10 mM, DmHKT1 S84G-mediated inward K^+ currents were twice as high as those of Na^+. In the presence of Na^+ and K^+, current amplitudes were additive (Figure 3C). This indicates that in DmHKT1, the serine-to-glycine mutation alters the permeability of Na^+ relative to K^+.

To study the nature of sodium-potassium interdependence, we exposed DmHKT1 S84G to a stepwise increase in sodium concentration in the presence of 10 mM extracellular potassium. With increasing sodium concentrations, the wild-type Na^+ conductance showed a saturation curve with a $K_m(Na^+)$ of 44.0 ± 4.4 mM, while the Na^+ conductance of the mutant channel increased linearly (Figure 3D).

The Na^+ conductance of wild-type DmHKT1 was largely unaffected when the Na^+ was at constant levels alongside a variable external K^+ content. However, the serine-to-glycine mutant exhibited a saturation curve defined by a $K_m(K^+)$ value of 23.5 ± 7.24 mM (Figure 3E). A constant Na^+ concentration of 10 mM increased the $K_m(K^+)$ 2.6-fold over the $K_m(K^+)$ value (9.01 ± 1.99 mM) obtained with pure K^+ solutions (Figure 3B). Interestingly, under these conditions we did not observe the self-inhibition of DmHKT1 S84G; this could only be found in the sodium-free K^+ solution (Figure 3B). These observations lead to the conclusion that, because of the weak sodium conductance in the mutant, the presence of this ion hinders potassium from passing the pore.

The Pore Serine Residue Is Key for Sodium Selectivity of DmHKT1

To study ion permeation through the Na^+/K^+-permeable DmHKT1 mutant S84G, we used an approach based on the anomalous mole fraction effect (AMFE) for both alkali cations (Figure 3F). We tested DmHKT1 S84G, which, as shown above, is permeable to both Na^+ and K^+ ions. In this approach, the total concentration of the mixture ([Na^+] plus [K^+]) is fixed to 50 mM, while the mole fraction [Na^+]/([Na^+] plus [K^+]) is altered (Takeuchi and Takeuchi, 1971; Neher, 1975). The current through the pore of DmHKT1 S84G measured is mediated by the motion of the ions through the selectivity filter. For some channels, the conductance of the mixture is lower than the end-point conductance for single ions, which is described as AMFE. Nonetheless, in the *Dionaea* DmHKT1 S84G, a linear decrease

in influx was observed when 50 mM K^+ was continuously replaced by Na^+ (Figure 3F), and no AMFE was detectable. This finding indicates that the pore of the DmHKT1 channel contains a maximum of one ion at a time, as opposed to allowing K^+ and Na^+ to interact during the pore transition process by sharing binding sites. Thus, the nature of the side chain at position 84 is key to the selectivity filter of DmHKT1. The serine in the *Dionaea* wild-type channel restricts alkali metal cation permeation to Na^+, while a glycine residue at this position leads to preferential K^+ permeation. Consequently, it can be concluded that the glycine residue found in the pore of subfamily two of HKT1-like molecules leads to a higher affinity for K^+ than Na^+ in these transporters.

To gain first structural insights into the architecture of the selectivity filter in DmHKT1, we calculated the binding-site location for the monovalent cation as described by Scherzer et al. (2013). Assuming a single binding site, as indicated by the Michaelis–Menten kinetics of DmHKT1 S84G (Figure 3B), and a K^+ concentration at this point that is in electrochemical equilibrium with the bath medium, we located the K^+-binding site in DmHKT1 S84G at ($\delta = 0.37 \pm 0.012$) 37% within the membrane electrical field relative to the extracellular face of the *Dionaea* channel (Figure 4A, insert). To study the alkali metal binding site(s) in the pore of wild-type DmHKT1 and the mutant S84G in more detail, we performed homology modeling using the structure of the bacterial Trk/Ktr/HKT ion channel KtrAB from *Bacillus subtilis* (Vieira-Pires et al., 2013) as a template. In contrast to the classical K^+ ion channels of the KcsA family, which comprise four identical subunits, Trk/Ktr/HKT-type ion channels consist of one single chain; thus the pore, built from four loops, is inherently asymmetric. Analysis of the pore signature from the KtrB template structure of *B. subtilis*, however, reveals four-fold pseudo-symmetry with an apparently invariant glycine residue present in all four pore-lining loops close to the extracellular entrance of the channel. In contrast to K^+ ion channels of the KcsA family, HKT ion channels contain only one metal ion coordination site in the pore formed by a double ring of main-chain carbonyl groups located on the four pore loops (Figure 4A–4E), as is apparent in the structure of *B. subtilis* KtrB (PDB: 4J7C). Using our model of DmHKT1 (Figure 4A), the metal ion coordination site in the pore can be estimated at 35% within the membrane viewed from the channel's extracellular face. Thus, the electrophysiological and structural approaches consistently locate the selectivity filter at the same position (Figure 4A). Close to this spot, the homology modeling also showed that the central glycine residue, which is present in the first pore loop of the template KtrB, is replaced by a serine, ultimately affecting the pore geometry and, hence, metal ion coordination (Figure 4B–4D). Modeling suggests two possible orientations for serine 84: one where the side-chain hydroxyl group is inside the Na^+-conducting pore (Figure 4C), and the other where it points away from the pore interior. To test whether the orientation of the hydroxyl group is key for Na^+/K^+ discrimination, we introduced an alanine into position 84 (Figure 4E). The small alanine lacks the polar side-chain hydroxyl group, but in contrast to a glycine residue it nevertheless enforces the channel to adopt the same backbone conformation within the metal-coordinating double carbonyl ring, as with serine (Figure 4E and Supplemental Figure 3). The DmHKT1 mutant S84A, when expressed in *Xenopus* oocytes, was still permeable to Na^+ and K^+, similar to the mutant S84G. However, the K^+ influx was only half that observed with S84G (Figure 4F). These findings suggest that the hydroxyl group of the serine residue of wild-type DmHKT1 does indeed participate in cation selection, and is therefore likely to be oriented into the pore interior.

DISCUSSION

DmHKT1 Is Designed to Serve as a Sodium-Selective Channel

A mole fraction experiment is a very powerful tool for determining whether only one ion occupies the selectivity filter at a time, or whether the selectivity filter can hold several ions that then interfere with each other during ion channeling in the pore. An AMFE is usually interpreted in a multi-ion model where different ions compete for multiple binding sites, often resulting in flux coupling (Hille, 1992). Our finding of the absence of an AMFE shows that the channel contains, at most, only a single ion at a time. Together, our combined molecular modeling and mutational analysis on DmHKT1 and structural data available for other members of the HKT family provided insights into how ion selectivity in this channel family is achieved (see also Supplemental Figure 2). Ion channel isoforms of this family, which are capable of transporting potassium, share four glycine residues in the center of the four pore-lining loops. The special backbone conformation introduced into the loop segments by these glycine residues allows the formation of two stacked main-chain carbonyl rings, which yields a potassium-selective metal-coordination site. In contrast to those isoforms, DmHKT1, in which the first pore loop harbors a serine residue instead, is highly sodium selective. The exchange of Ser84 in the first pore loop of DmHKT1 renders the fully sodium-selective DmHKT1 into an HKT isoform that does not further discriminate between sodium and potassium (Figure 3A). This strongly indicates that the hydroxyl group of the serine residue is an integral part of the sodium coordination. Since in our homology model the side chain of S84 faces the pore interior, its hydroxyl group possibly acts as an additional "water-like" coordination group (Figure 4C) similar to what was proposed for analogous KtrB variants also showing an increased Na^+/K^+ selectivity (Tholema et al., 2005). However, rather than a size-restrained ion selectivity mechanism due to narrowing of the pore by the serine side chain as proposed by Tholema et al. (2005), we suggest that the change in the carbonyl ring geometry together with the additional hydroxyl group results in a metal ion-binding site with a coordination number between 5 and 6. This altered geometry with a lower coordination number seems, then, to provide a perfect selection filter for sodium over potassium. For a more detailed description of the selectivity filter, see also Supplemental Text S1.

The *Dionaea* Trap Na^+ Channel Is Capable of Processing Prey-Derived Sodium Loads

While K^+ is the most abundant cation in the cytoplasm of plant cells, typically reaching about 100 mM, Na^+ is highly toxic even at low-mM cytosolic concentrations (Kingsbury and Epstein, 1986; Luan et al., 2009). The key to salt tolerance is to sequester the Na^+ taken up by the plant to the vacuoles or transfer it to older tissues (Blumwald, 2000; Munns and Tester, 2008). In a parallel study we have shown that stimulated flytraps take up and accumulate prey-derived sodium via

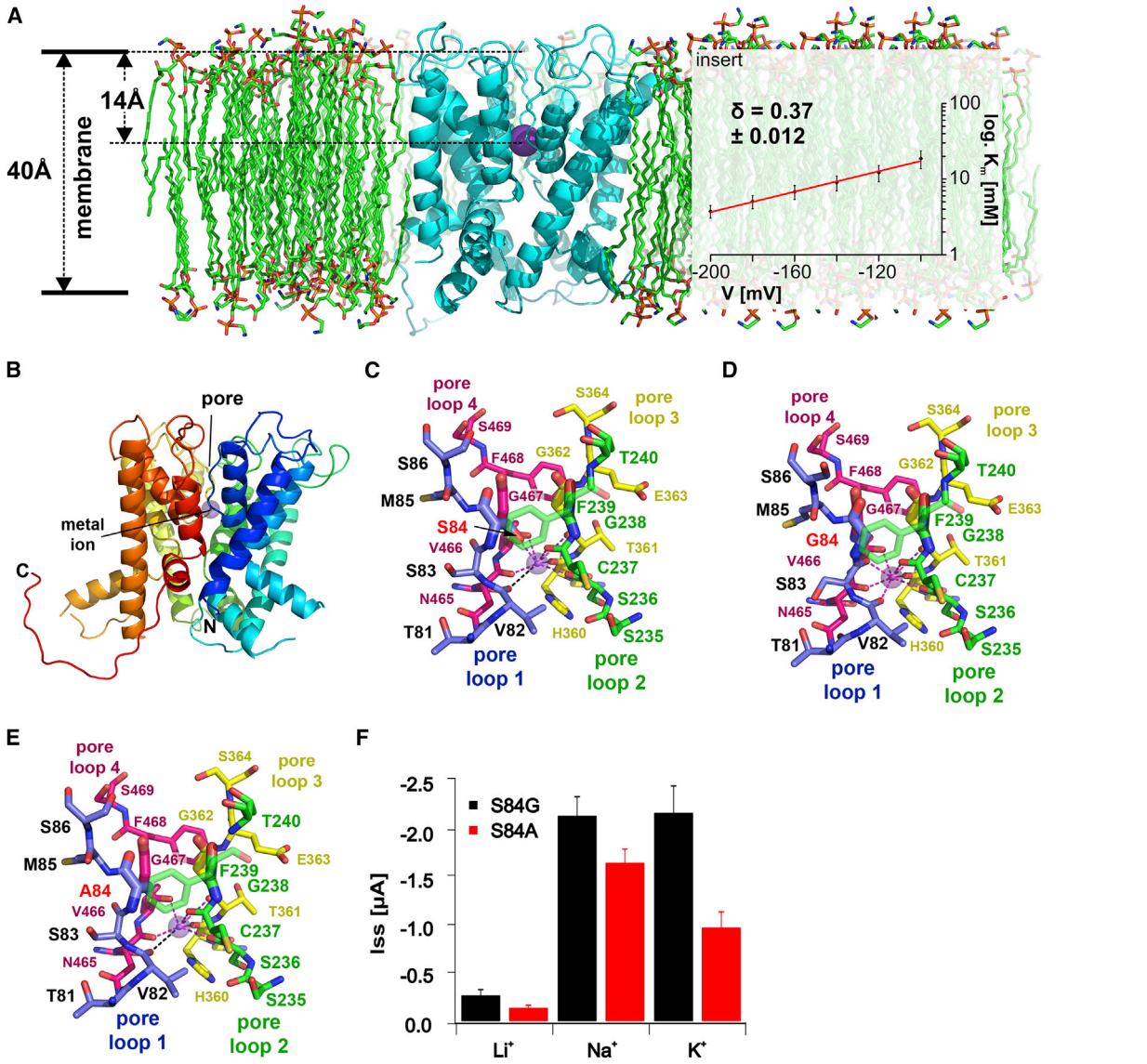

Figure 4. Homology Modeling of the DmHKT1 Pore.

(A) DmHKT1 channel (ribbon plot in cyan) embedded in an artificial phosphatidylethanolamine (POPE) membrane bilayer (lipid molecules shown as stick representation). The model of DmHKT1 was placed in the bilayer using the ProBML web server (http://compbio.clemson.com/problm_webserver). The thickness of the membrane bilayer and the distance between the potassium ion (magenta sphere) in the selectivity filter and the upper boundary of the membrane were measured with Quanta2008. The insert shows the K_m dependency of DmHKT1 S84G on clamped voltage. Data were fitted with an exponential function ($K_m = K_{m0} \exp[\delta z F V_m / RT]$). Since $zF/RT = 0.0417\ mV^{-1}$, the resulting parameters were $K_{m0} = 139.46 \pm 11.54$ mM and $\delta = 0.370 \pm 0.012$ ($n = 6$). Currents and voltages were recorded with standard bath solution containing indicated K^+ concentrations.

(B) 3D homology model of the *D. muscipula* ion channel DmHKT1 shown as ribbon plot with the chain colored from blue (N terminus) to red (C terminus). The pore and metal-binding site are indicated.

(C) Magnification of the four pore-lining loops of wild-type DmHKT1 with the carbon atoms colored blue (loop 1, amino acids [aa] Thr81 to Ser86), green (loop 2, aa Ser235 to Thr240), yellow (loop 3, aa Arg359 to Ser364), and red (loop 4, aa Gly464 to Ser469). The hydroxyl group of serine 84 is located inside the pore lumen and participates in the coordination of the sodium ion (magenta sphere). Stippled lines indicate the metal ion coordination by the surrounding carbonyl groups of Val82, Ser236, Val237, His360, Thr361, Asn465, and Val466, and the hydroxyl group of Ser84. The distance between the carbonyl group of Val82 and the metal ion exceeds 3.2 Å, and therefore may not contribute to metal coordination (black stippled line).

(D) Magnification of the DmHKT1 variant with a glycine residue occupying position 84 (S84G). The exchange of serine 84 in the first pore-lining loop by glycine results in altered backbone conformation of the preceding amino acid residues Ser83 and Val82 (see also Supplemental Figure 3), thereby reorienting their carbonyl groups toward the metal coordination site in the pore. This conformation is also found in potassium-conducting bacterial ion channels of this channel family, e.g. TrkH and KtrB, suggesting that pore loops containing a central glycine residue can adopt favorable backbone conformations for enhanced potassium binding.

(legend continued on next page)

Dionaea sodium channels, which operate in gland cells (Böhm et al., 2016). The sodium intake and storage in the trap parenchyma of carnivorous *Dionaea* is reminiscent of the salt management of the succulent halophytes (Shabala et al., 2014). Depending on the salinity to which the green stomach is exposed, glands depolarize, resulting in APs (Figure 1A and 1B), the same type of electrical signal initiated when prey animals accidentally touch the trigger of the Darwin plant (Escalante-Perez et al., 2011). Generated in the trigger hair mechanosensor, these APs travel along the lobe surface to excite the motor unit and the glands (Escalante-Perez et al., 2011). In animal axons, APs depend on inward-flowing Na^+ (depolarization), but in *Dionaea*, sodium ions in general and DmHKT1-based Na^+ channeling in particular are unlikely to contribute to the APs. This notion is manifested by the fact that even high Na^+ levels do not significantly change the AP shape and amplitude (Figure 1C). In other words, in *Dionaea*, the AP itself is salt insensitive; rather, the carnivorous plant consuming sodium-rich animals seems to take advantage of Na^+ intake for maintaining cellular osmotic potential and turgor just like halophytes (Shabala, 2011).

Why Do High Saline Loads Induce Self-Sustained Oscillatory Electrical Activity?

The resting potential of non-stimulated traps is in the range of −120 to −140 mV. Upon high saline stimulation, entry of Na^+ via DmHKT1 shifts the membrane toward the threshold (around −100 mV [Beilby, 2007]) of the *Dionaea* AP. In the "pacemaker mode," inward Na^+ currents keep the membrane in firing mode. This repetitive firing of APs prevents the flytrap from Na^+ influx-dependent, long-term depolarization. Positively charged Na^+ entering the cell is counteracted by a SKOR/GORK-type channel (for review see Hedrich, 2012), which mediates an outward flux of positively charged K^+. This *in toto* electroneutral cation exchange keeps the membrane potential hyperpolarized. Such a function can only be fulfilled by the Na^+-selective DmHKT1 channel, since Na^+/K^+-permeable isoforms, present in bacteria and many plant species, would interfere with the AP in the flytrap and with the information management it requires to hunt for animals to obtain its nutrient supply.

METHODS

Modeling of DmHKT1

Structures of wild-type DmHKT1 and the mutants S84G and S84A were obtained by homology modeling using the structure of the bacterial Trk/Ktr/HKT ion channel KtrAB from *B. subtilis* (Vieira-Pires et al., 2013) (PDB: 4J7C). The structure of the bacterial template KtrAB was determined with the ion channel unit KtrB in complex with its cytosolic regulatory subunit KtrA. The ion channel forms a hetero-octameric assembly in the asymmetric unit of the crystal, with two KtrB channel dimers and four regulatory subunits, KtrA, bridging the two ion channel dimers (Vieira-Pires et al., 2013). As no regulatory subunit corresponding to KtrA exists for DmHKT1, and no information is available as to whether DmHKT1 also forms dimers, one protein chain (chain I) of the template (PDB: 4J7C) was selected for homology modeling. An amino acid sequence alignment was performed using the sequences of DmHKT1, the selected structure template, and other plant and bacterial HKT ion channels from rice, wheat, barley, reed, *Arabidopsis*, succulents, and *Escherichia coli*, and by employing the software ClustalW2. The DmHKT1 monomer was then modeled on the basis of the template structure of KtrB by replacing the amino acids that differed in the sequence alignment using the tool ProteinDesign from the software package Quanta2008 (Accelrys, San Diego).

The KtrB monomer is built from four repeats. Each repeat consists of a long transmembrane helix M1, a 3.5-turn pore helix with the subsequent pore loop forming the selectivity filter, and a second transmembrane helix M2, which in repeats 1, 2, and 4 is kinked in the middle by almost 90°, the result of a conserved two-amino-acid motif that contains at least one glycine. In repeat 3 of the template KtrB, helix M2 has a large glycine-/serine-rich insertion forming a bulged-out loop. This is missing in DmHKT1 and is replaced by a double proline motif. Insertions and deletions (compared with the template) found in the loops between helix M1 and the pore helix of all four repeats of DmHKT1, as well as the bulged loop of helix M2 of repeat 3, were modeled manually. Larger insertions, as found in the transition loops of helix M2 of one repeat to the M1 helix of the next repeat (as found between repeats 1 and 2, and between repeats 2 and 3) were not modeled. Backbone torsion angles were restrained to obey angles within the allowed region of the Ramachandran plot when possible. If present, incorrect van der Waals contacts were eliminated first by performing side-chain rotamer searches using the tool Xbuilt in the software Quanta2008. Final refinement involved a stepwise energy-minimization routine whereby all backbone atoms were first kept fixed and side-chain atoms were restrained by a soft harmonic potential (E_{harm} = 10 kcal mol^{-1} $Å^{-2}$). In subsequent steps, the harmonic potential was gradually decreased to zero. In the final minimization step, the backbone atoms were restrained by a harmonic potential (E_{harm} = 20 kcal mol^{-1} $Å^{-2}$) and energy minimization was performed until the Lennart–Jones energy was negative, indicating the absence of van der Waals clashes. Only geometrical terms were used because the energy-minimization procedure did not implement solvent molecules for proper treatment of electrostatics.

Plant Material and Tissue Sampling

D. muscipula plants were purchased from CRESCO Carnivora (the Netherlands) and grown in plastic pots at 22°C with a 16:8-h light/dark photoperiod. For induction of digestion, 100 μM COR solution (Sigma-Aldrich, Germany) was directly applied to the respective tissues, and samples were used after 24 h.

Non-Invasive Ion Flux Measurements

Net fluxes of Na^+ and K^+ were measured using the non-invasive MIFE technique (University of Tasmania, Australia). The theory of non-invasive MIFE measurements and all specific details of microelectrode fabrication and calibration are available in our prior publications (Shabala et al., 1997, 2006; Shabala and Shabala, 2002). In brief, microelectrodes with an external tip diameter of ~2 μm were pulled, salinized, and filled with either K^+-selective cocktail (K^+ 60031, Sigma) or with a highly Na^+- selective resin that is not responsive to K^+ (Jayakannan et al., 2011). Electrodes were calibrated to an appropriate set of standards and mounted on a 3D micromanipulator (MMT-5; Narishige, Toyko, Japan). An immobilized lobe was placed into a 90-mm Petri dish containing 40 ml of basic salt medium (BSM: 0.2 mM KCl, 0.1 mM $CaCl_2$, adjusted to the required pH using 2-(*N*-morpholino)

(E) Magnification of a mutant ion channel DmHKT1 with alanine at position 84 (S84A). The metal coordination is supposedly similar to wild-type DmHKT1 carrying a serine residue at this position. However, the missing serine hydroxyl group, hence the lack of one metal coordination site, impairs the Na^+–K^+ discrimination.

(F) Steady-state currents (Iss) of DmHKT1 S84G (black) and DmHKT1 S84A expressing oocytes at −140 mV and in 100 mM of the indicated cations (n = 4, mean ± SD).

ethanesulfonic acid [MES]/Tris) and placed into a Faraday cage. Na^+- and K^+-selective microelectrodes were positioned, with their tips aligned, 50 μm above the lobe surface using a 3D hydraulic manipulator. During measurements, a computer-controlled stepper motor moved electrodes in a slow (10 s) square-wave cycle between the two positions, close to (50 μm) and away from (150 μm) the trap surface. The potential difference between two positions was recorded by the MIFE CHART software (Shabala et al., 1997) and converted to an electrochemical potential difference using the calibrated Nernst slopes of the electrodes. Net ion fluxes were calculated using the MIFEFLUX software for cylindrical diffusion geometry (Newman, 2001).

To study the dose dependence of Na^+ uptake, intact *Dionaea* leaves were pre-treated with coronatine for 24 h as described above. A single lobe was cut and immobilized in a measuring chamber by using medical adhesive (VH355; Ulrich AG, St Gallen, Switzerland). The lobe was left to equilibrate in BSM solution before flux measurements commenced. Net Na^+ and K^+ fluxes were measured in response to the successive increase in the NaCl content of the external BSM (NaCl: 0, 3, 10, 50 mM) for 3 min at each NaCl concentration. The pH of the media was maintained at 5 or 4, and pH 8 in Figure 2B. Traps without COR treatment were used as controls.

Surface Potential Measurements

To quantify APs in the Venus flytrap, we used no invasive surface potential electrodes. One Ag/AgCl wire was fixed with tape to the outer trap surface, and electrical connection was improved by applying a droplet of Kontakt-Gel (Labokinika, Rottenburg, Germany). The reference Ag/AgCl electrode was put into the wet soil. Electrical signals were amplified 100-fold and recorded with PatchMaster software (HEKA, Lambrecht, Germany). The standard solution containing 0.1 mM KCl, 10 mM $CaCl_2$ and 15 mM MES, adjusted with Tris to pH 6, was kept at 1060 mOsm/kg with D-sorbitol when required. The concentrations of NaCl used to supplement the standard solution were 0 mM and 510 mM (3%).

Intracellular Measurements

Prior to measurements, the lobe of a cut trap was glued to a chamber bottom and left for recovery (30 min) in a standard solution containing 0.1 mM KCl, 10 mM $CaCl_2$, and 15 mM MES, adjusted with Tris to pH 6, or 15 mM Tris, adjusted with MES to pH 4. Osmolarity was kept at 240 mOsm/kg with D-sorbitol when required. The concentrations of NaCl used to supplement the standard solution were 60, and 510 mM (3%). During experiments leaves were continuously perfused with the standard solution (1 ml/min). For stimulation, a 1-min exposure to the respective NaCl concentration was sufficient.

Oocyte Recordings

For double-electrode voltage-clamp studies, oocytes were perfused with Tris/MES-based buffers. The standard bath solution contained 10 mM Tris/MES (pH 5.6), 1 mM $CaCl_2$, 1 mM $MgCl_2$ and 1 mM $LaCl_3$, osmolality adjusted to 220 mOsm/kg with D-sorbitol. Lithium was used to balance the ionic strength for measurements under varying cation (Na^+ and K^+) concentrations. Solutions for selectivity measurements were composed of the standard bath solution supplemented with 100 mM Na^+, $NMDG^+$ (*N*-methyl-D-glucamine), Li^+, K^+, Rb^+, or Cs^+ chloride salts. For current–voltage relations (*IV* curves), single-voltage pulses were applied in 10-mV increments from −200 to +60 mV, starting from a holding potential (V_H) of 0 mV. Steady-state currents (I_{SS}) were extracted at the end of the test pulses lasting 50 ms. Data were analyzed using Igor Pro and Origin Pro 9.0G.

SUPPLEMENTAL INFORMATION

Supplemental Information is available at *Molecular Plant Online*.

FUNDING

This work has been supported by the European Research Council under the European Union's Seventh Framework Program (FP/20010-2015)/ERC Grant Agreement no. [250194-Carnivorom]. This work was also supported by the International Research Group Program (IRG14-08), Deanship of Scientific Research, King Saud University, Saudi Arabia (E.N.), and by grants from the Australian Research Council (project DP150101663) and the Grain Research and Development Corporation (to S. Shabala.).

AUTHOR CONTRIBUTIONS

E.N. and R.H. conceived the work; S.S. and J.B. conducted initial feasibility studies; J.B., S.S., E.K., S. Shabala, E.N., T.D.M., and R.H. designed the experiments and analyzed the data; S.S., J.B., E.K., and T.D.M. performed the experiments; and S.S., E.N., T.D.M., and R.H. wrote the manuscript.

ACKNOWLEDGMENTS

No conflict of interest declared.

Received: August 18, 2015
Revised: September 24, 2015
Accepted: September 24, 2015
Published: October 5, 2015

REFERENCES

Ali, Z., Park, H.C., Ali, A., Oh, D.H., Aman, R., Kropornicka, A., Hong, H., Choi, W., Chung, W.S., Kim, W.Y., et al. (2012). TsHKT1;2, a HKT1 homolog from the extremophile *Arabidopsis* relative *Thellungiella salsuginea*, shows K(+) specificity in the presence of NaCl. Plant Physiol. **158**:1463–1474.

Balotin, N.M., and Dipalma, J.R. (1962). Spontaneous electrical activity of *Dionaea muscipula*. Science **138**:1338–1339.

Beilby, M.J. (2007). Action potential in charophytes. Int. Rev. Cytol. **257**:43–82.

Blumwald, E. (2000). Sodium transport and salt tolerance in plants. Curr. Opin. Cell. Biol. **12**:431–434.

Böhm, J., Scherzer, S., Krol, E., Kreuzer, I., von Meyer, K., Lorey, C., Mueller, T.D., Shabala, L., Monte, I., Solano, R., et al. (2016). The Venus flytrap Dionaea muscipula counts prey-induced action potentials to induce sodium uptake. Curr. Biol. **21**, http://dx.doi.org/10.1016/j.cub.2015.11.057.

Corratge-Faillie, C., Jabnoune, M., Zimmermann, S., Very, A.A., Fizames, C., and Sentenac, H. (2010). Potassium and sodium transport in non-animal cells: the Trk/Ktr/HKT transporter family. Cell. Mol. Life Sci. **67**:2511–2532.

Escalante-Perez, M., Krol, E., Stange, A., Geiger, D., Al-Rasheid, K.A.S., Hause, B., Neher, E., and Hedrich, R. (2011). A special pair of phytohormones controls excitability, slow closure, and external stomach formation in the Venus flytrap. Proc. Natl. Acad. Sci. USA **108**:15492–15497.

Escalante-Perez, M., Scherzer, S., Al-Rasheid, K.A.S., Dottinger, C., Neher, E., and Hedrich, R. (2014). Mechano-stimulation triggers turgor changes associated with trap closure in the Darwin plant *Dionaea muscipula*. Mol. Plant **7**:744–746.

Forterre, Y., Skotheim, J.M., Dumais, J., and Mahadevan, L. (2005). How the Venus flytrap snaps. Nature **433**:421–425.

Gao, P., Loeffler, T.S., Honsel, A., Kruse, J., Krol, E., Scherzer, S., Kreuzer, I., Bemm, F., Buegger, F., Burzlaff, T., et al. (2015). Integration of trap- and root-derived nitrogen nutrition of carnivorous *Dionaea muscipula*. New Phytol. **205**:1320–1329.

Gomez-Porras, J.L., Riano-Pachon, D.M., Benito, B., Haro, R., Sklodowski, K., Rodriguez-Navarro, A., and Dreyer, I. (2012). Phylogenetic analysis of K(+) transporters in bryophytes, lycophytes, and flowering plants indicates a specialization of vascular plants. Front. Plant Sci. **3**:167.

Hauser, F., and Horie, T. (2010). A conserved primary salt tolerance mechanism mediated by HKT transporters: a mechanism for sodium exclusion and maintenance of high K(+)/Na(+) ratio in leaves during salinity stress. Plant Cell Environ. **33**:552–565.

Hedrich, R. (2012). Ion channels in plants. Physiol. Rev. **92**:1777–1811.

Hille, B. (1992). Ionic Channels of Excitable Membranes, 2nd edn (Sunderland: Sinauer Associates Inc).

Horie, T., Brodsky, D.E., Costa, A., Kaneko, T., Lo Schiavo, F., Katsuhara, M., and Schroeder, J.I. (2011). K(+) transport by the OsHKT2;4 transporter from rice with atypical Na(+) transport properties and competition in permeation of K(+) over Mg(2+) and Ca(2+) ions. Plant Physiol. **156**:1493–1507.

Jayakannan, M., Babourina, O., and Rengel, Z. (2011). Improved measurements of Na(+) fluxes in plants using calixarene-based microelectrodes. J. Plant Physiol. **168**:1045–1051.

Kingsbury, R.W., and Epstein, E. (1986). Salt sensitivity in wheat: a case for specific ion toxicity. Plant Physiol. **80**:651–654.

Kreuzwieser, J., Scheerer, U., Kruse, J., Burzlaff, T., Honsel, A., Alfarraj, S., Georgiev, P., Schnitzler, J.P., Ghirardo, A., Kreuzer, I., et al. (2014). The Venus flytrap attracts insects by the release of volatile organic compounds. J. Exp. Bot. **65**:755–766.

Kruse, J., Gao, P., Honsel, A., Kreuzwieser, J., Burzlaff, T., Alfarraj, S., Hedrich, R., and Rennenberg, H. (2014). Strategy of nitrogen acquisition and utilization by carnivorous *Dionaea muscipula*. Oecologia **174**:839–851.

Lan, W.Z., Wang, W., Wang, S.M., Li, L.G., Buchanan, B.B., Lin, H.X., Gao, J.P., and Luan, S. (2010). A rice high-affinity potassium transporter (HKT) conceals a calcium-permeable cation channel. Proc. Natl. Acad. Sci. USA **107**:7089–7094.

Luan, S., Lan, W., and Chul Lee, S. (2009). Potassium nutrition, sodium toxicity, and calcium signaling: connections through the CBL-CIPK network. Curr. Opin. Plant Biol. **12**:339–346.

Mian, A., Oomen, R.J., Isayenkov, S., Sentenac, H., Maathuis, F.J., and Very, A.A. (2011). Over-expression of an Na(+)-and K(+)-permeable HKT transporter in barley improves salt tolerance. Plant J. **68**:468–479.

Munns, R., and Tester, M. (2008). Mechanisms of salinity tolerance. Annu. Rev. Plant Biol. **59**:651–681.

Neher, E. (1975). Ionic specificity of gramicidin channel and thallous ion. Biochim. Biophys. Acta **401**:540–544.

Newman, I.A. (2001). Ion transport in roots: measurement of fluxes using ion-selective microelectrodes to characterize transporter function. Plant Cell Environ. **24**:1–14.

Platten, J.D., Cotsaftis, O., Berthomieu, P., Bohnert, H., Davenport, R.J., Fairbairn, D.J., Horie, T., Leigh, R.A., Lin, H.X., Luan, S., et al. (2006). Nomenclature for HKT transporters, key determinants of plant salinity tolerance. Trends Plant Sci. **11**:372–374.

Rubio, F., Gassmann, W., and Schroeder, J.I. (1995). Sodium-driven potassium uptake by the plant potassium transporter HKT1 and mutations conferring salt tolerance. Science **270**:1660–1663.

Schachtman, D.P., and Schroeder, J.I. (1994). Structure and transport mechanism of a high-affinity potassium uptake transporter from higher plants. Nature **370**:655–658.

Scherzer, S., Krol, E., Kreuzer, I., Kruse, J., Karl, F., von Ruden, M., Escalante-Perez, M., Muller, T., Rennenberg, H., Al-Rasheid, K.A., et al. (2013). The *Dionaea muscipula* ammonium channel DmAMT1 provides NH(4+) uptake associated with Venus flytrap's prey digestion. Curr. Biol. **23**:1649–1657.

Scherzer, S., Bohm, J., Krol, E., Shabala, L., Kreuzer, I., Larisch, C., Bemm, F., Al-Rasheid, K.A., Shabala, S., Rennenberg, H., et al. (2015). Calcium sensor kinase activates potassium uptake systems in gland cells of Venus flytraps. Proc. Natl. Acad. Sci. USA **112**:7309–7314.

Shabala, S. (2011). Physiological and cellular aspects of phytotoxicity tolerance in plants: the role of membrane transporters and implications for crop breeding for waterlogging tolerance. New Phytol. **190**:289–298.

Shabala, S., and Shabala, L. (2002). Kinetics of net H(+), Ca(2+), K(+), Na(+), NH(4+), and Cl(-) fluxes associated with post-chilling recovery of plasma membrane transporters in *Zea mays* leaf and root tissues. Physiol. Plant. **114**:47–56.

Shabala, S.N., Newman, I.A., and Morris, J. (1997). Oscillations in H(+) and Ca(2+) ion fluxes around the elongation region of corn roots and effects of external pH. Plant Physiol. **113**:111–118.

Shabala, S., Demidchik, V., Shabala, L., Cuin, T.A., Smith, S.J., Miller, A.J., Davies, J.M., and Newman, I.A. (2006). Extracellular Ca(2+) ameliorates NaCl-induced K(+) loss from *Arabidopsis* root and leaf cells by controlling plasma membrane K(+) -permeable channels. Plant Physiol. **141**:1653–1665.

Shabala, S., Bose, J., and Hedrich, R. (2014). Salt bladders: do they matter? Trends Plant Sci. **19**:687–691.

Sheng, S.H., and Kleyman, T.R. (2003). External Cd(2+) accessibility of introduced sulfhydryl groups at the selectivity filter of the epithelial Na(+) channel. Biophys. J. **84**:530a.

Takeuchi, A., and Takeuchi, N. (1971). Anion interaction at the inhibitory post-synaptic membrane of the crayfish neuromuscular junction. J. Physiol. **212**:337–351.

Tholema, N., Vor der Bruggen, M., Maser, P., Nakamura, T., Schroeder, J.I., Kobayashi, H., Uozumi, N., and Bakker, E.P. (2005). All four putative selectivity filter glycine residues in KtrB are essential for high affinity and selective K(+) uptake by the KtrAB system from *Vibrio alginolyticus*. J. Biol. Chem. **280**:41146–41154.

Vieira-Pires, R.S., Szollosi, A., and Morais-Cabral, J.H. (2013). The structure of the KtrAB potassium transporter. Nature **496**:323–328.

Waters, S., Gilliham, M., and Hrmova, M. (2013). Plant high-affinity potassium (HKT) transporters involved in salinity tolerance: structural insights to probe differences in ion selectivity. Int. J. Mol. Sci. **14**:7660–7680.